A Novel Hybrid Swarm Intelligence and Cuckoo Search Based Microgrid EMS for Optimal Energy Scheduling

Priyadarshini Balasubramanyam* and Vijay K. Sood

Faculty of Engineering and Applied Science, Ontario Tech University, Oshawa, ON L1G 0C5, Canada
E-mail: Priyadarshini.balasubramanyam1@ontariotechu.net
**Corresponding Author*

Received 30 August 2022; Accepted 28 November 2022;
Publication 16 May 2023

Abstract

A grid-connected or islanded microgrid made up of distributed energy sources (DERs), requires a power management/dispatch system to control the power dispatch and meet the load demand in the system. At the tertiary control level in a typical microgrid, an optimal scheduling mechanism is used to manage the power generated from the local DERs, energy drawn from the grid and energy consumption by the load. This paper proposes a novel hybrid optimization technique for day-ahead scheduling in a smart-grid. A Hybrid Feedback PSO-MCS algorithm is implemented using swarm intelligence and cuckoo search to enhance the performance and obtain a cost-effective solution for a microgrid prosumer. A comparison has been made of the Hybrid Feedback PSO-MCS (HFPSOMCS) algorithm with PSO and modified CS (MCS) algorithm. The best performing algorithm among the three is executed in MATLAB/Simulink and Python IDE platforms to compare the execution time.

Keywords: Microgrid, PSO, CSA, hybrid algorithm, optimization, EMS, tertiary control.

Distributed Generation & Alternative Energy Journal, Vol. 38_4, 1119–1148.
doi: 10.13052/dgaej2156-3306.3843

1 Introduction

Microgrids, an important component of modern power systems, have been rapidly evolving over the past two decades, with the goal of reaching net zero in the coming decades [1]. Economic operation of the networks besides maintaining high energy production efficiency have been the major focus areas. Several strategies aiming to minimize the overall microgrid costs through economic dispatch have been dis-cussed in [2–5].

Electricity/Utility sector has seen significant changes because of worldwide technology advancements. Solar PV and wind energy farms are gaining momentum be-cause of their widespread availability and the promise to offer an environmentally beneficial solution for the long-term sustainable electricity requirements of the future. These resources fluctuate widely, necessitating efficient and responsive power generation systems. Smart grid concepts play a crucial role in these transformations. The main problem is developing a Distributed Generator (DG) system for remote places. Presently, 17% of the world's population lacks access to electricity, according to recent figures. These regions are often served by diesel generators, which is not only expensive but also produces a large amount of environmental pollution. In this case, a hybrid system made up of one or more renewable energy sources or the idea of a localized generation (microgrid) has the potential to supply electricity eco-nomically.

With an ever-increasing global population and correspondingly higher electricity demands, power & automation engineers/researchers are investigating the potential of renewable energy sources. The installed capacity of renewables has grown drastically over the last several years. Due to falling PV panel prices, abundance of solar energy, government issued incentives and installation of such farms and roof top models, the usage of renewables has experienced a significant uptick. It is difficult to regulate the fluctuating nature of the renewables while still incorporating it into an overall microgrid system. However, there are several advantages to doing so.

References [6–8] give an overview of the literature on energy management systems (EMSs) that include renewable energy sources. An in-depth analysis of the EMS is discussed in [9] giving a detailed study of optimum energy dispatch. EMS in islanding mode is optimized using methods like Tabu Search [10], dynamic programming [11], Particle Swarm Optimization (PSO) [12, 13], and hybrid PSO Fuzzy Logic [14]. Astitva et al. provided a novel EMS for a microgrid with extensive focus on PV penetration and battery energy storage systems in grid connected mode of operation.

A modified Grey Wolf Optimization technique was used for microgrid control and facilitate the economic dispatch of DERs [15].

EMS in a microgrid participates in optimization, planning & scheduling using several control strategies, programming methods, and a set of constraints. Its performance can be enhanced by using machine learning, deep learning, data science, data mining techniques/applications. A comprehensive and extensive review of the above-mentioned aspects of microgrids including advantages and disadvantages was studied in [16]. Battery energy storage systems (BESSs) are deployed into the hybrid microgrids to reduce fluctuations in power output, maintain main grid frequency, to alleviate transients in the system, and efficient storage of excess power [17].

A microgrid performs in an efficient manner with a robust EMS. In [18], the authors implemented a novel technique based on stochastic methods. Although, the strategy could handle the cost of operation and stand-by reserves, there was no technical investigation into microgrid's performance. Y. Li et al. [19] presented an autonomous nonlinear control strategy to enable smooth transitioning from grid-connected mode to islanded mode and vice versa. Multi objective optimization was implemented using a meta-heuristic algorithm called the ant colony optimization technique to obtain the optimal global solution. The system's goal is to reduce the amount of electricity purchased from the utility grid, hence increasing the local in-dependence.

This study applies a novel algorithm called HFPSOMCS to a microgrid with EMS in grid connected, islanded, and combined modes, considering a full day load fore-cast profile. Taking grid tariff rates and operational constraints into account, the proposed EMS monitored demand 24 hours a day, at the lowest operational cost for the DGs. When demand is high or when the microgrid's generation is insufficient to meet it, power can be purchased from the utility grid. If output exceeds demand during off-peak hours, electricity can be sold back to the main grid. The MG can supply electricity to important loads even when it is detached from the main grid. Testing the case studies using Texas Instruments C2000 microcontroller to send signals to the relays of the DGs is underway.

The rest of this paper is organized as follows. The microgrid modelling is presented in Section 2, and it contains schematics and mathematical functions of dis-tinct DERs and system boundaries. The implementation of optimization algorithms to the EMS system are discussed in Section 3. Section 4 throws light on simulation results for several case studies analysed during this work. Finally, Section 5 concludes the paper.

2 Microgrid Modelling

Figure 1 depicts the MG model that is utilized for the EMS and its corresponding schematic design. As part of this research, the conventional MG model is employed, which comprises several DGs, such as the Combined Heat & Power (CHP) plant, diesel generators (DG) and natural gas-fired generators (NGG). A PV system, Wind and Energy Storage Systems (ESS) are also included in this model. At the PCC, the DGs are linked and integrated to deliver electricity to the group of loads. Operationally, the MG may be used in three distinct ways:

- **Grid Connected Mode:** MG sells power back to the utility if generated power exceeds demand in this mode. MG purchases grid power when demand is greater than supply.

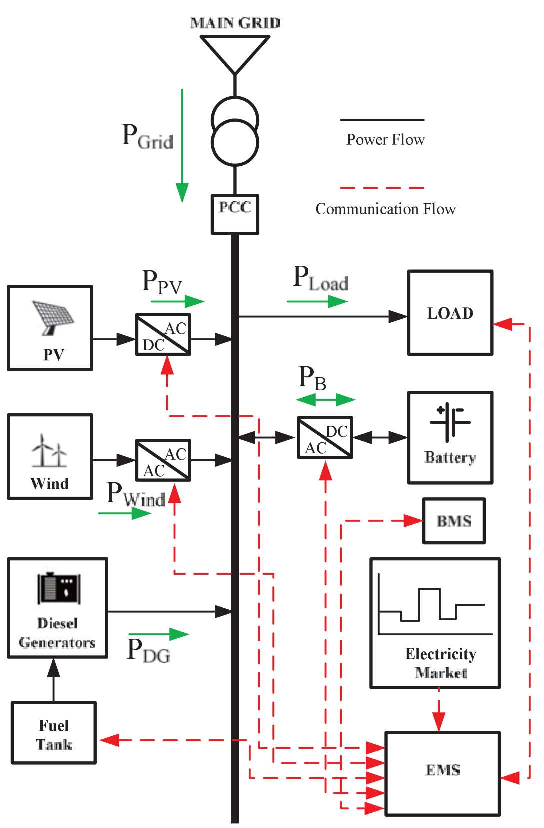

Figure 1 Schematic of the microgrid with EMS.

Table 1 Power ratings of the generators [28]

Lower Limit (MW) $\leq P_{Micro\ source} \leq$ Upper limit (MW)
$0 \leq P_{CHP} \leq 1.5$
$0 \leq P_{DG} \leq 1$
$0 \leq P_{NGG} \leq 1$
$0 \leq P_{PV} \leq 0.5$
$0 \leq P_{Wind} \leq 0.5$
$0.05 \leq P_{ESS} \leq 0.45$
$-1 \leq P_{Grid} \leq 1$

- **Islanded Mode:** When operating in this mode, the microgrid is cut off from the utility grid and only distributes electricity to the most essential loads. During this time, a process known as "load shedding" takes place to balance production and demand.
- **Combined Mode:** Due to a scheduled power outage, the system is running in grid connected mode on a certain day transition to islanded mode. As a result, the demand for power drops during these hours, allowing the EMS to determine the most cost-effective method of dispatching electricity to critical loads.

The power ratings of the system's distributed generators are shown in Table 1.

The mathematical modelling of each DG is formulated below as cost functions.

2.1 Fuel-fired Generators

Fuel costs for CHP, diesel generators, and natural gas generators may all be represented mathematically using the quadratic functions shown in Equation (1).

$$C_{Gen}(t) = \alpha_{Gen} + \beta_{Gen} P_{Gen}(t) + \gamma_{Gen} P_{Gen}^2(t) \tag{1}$$

Where α_{Gen}, β_{Gen}, and γ_{Gen} are the generator set's cost coefficients and the values considered for the study are tabulated below in Table 2 [26, 28].

2.2 PV

For a typical PV farm, the cost associated with generating and harnessing solar energy is given by

$$C_{PV}(t) = aI_P P_{PV}(t) + G^E P_{PV}(t) \tag{2}$$

Table 2 Cost coefficients settings of various DGs

DGs	α_{Gen}	β_{Gen}	γ_{Gen}
CHP	15.30	0.210	0.000240
Diesel Generator	14.88	0.300	0.000435
Natural Gas Generating Station	9.00	0.306	0.000315

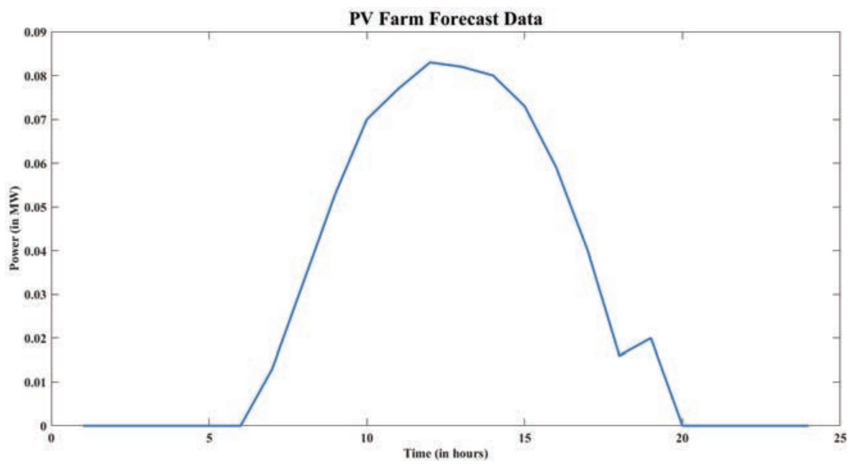

Figure 2 PV farm power forecast for 24 hours.

Where $P_{PV}(t)$ is the power generated by the farm in kW; I_P is the total investment cost per unit installed power ($/kW); G^E is cost of operation & maintenance ($/kW); a is coefficient of annuitization (no units) and it is calculated as follows:

$$a = \frac{r}{[1 - (1 + r)^{-N}]} \tag{3}$$

Where r is the rate of interest; N is investment period (=20 years). When calculating the entire cost of generating solar energy, it is important to consider the equipment's depreciation. Equations (2) and (3) are utilized to do this. The values for I_P and G^E are assumed to be $5000 and 1.6 cents/kW, respectively, in this case. As a result, it is possible to determine the ultimate cost function, which is shown by the Equation (4) [21, 28].

$$C_{PV}(t) = 545.016 \times P_{PV}(t) \tag{4}$$

Figure 2 illustrates the estimated power for this study's solar farm throughout a 24-hour period.

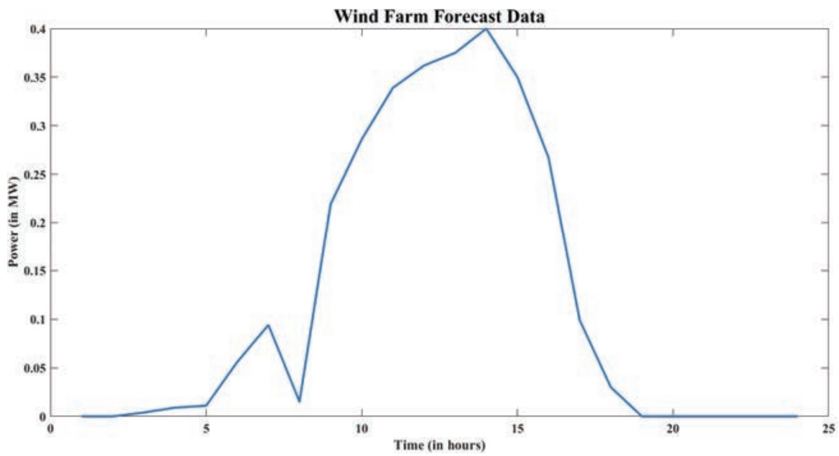

Figure 3 Wind farm power forecast for 24 hours.

2.3 Wind

Wind power's cost function is comparable to that of solar generation, according to Equations (2) and (3). However, I_P and G^E are estimated to be \$1400 and 1.6 cents/kW [28], respectively. As a result, the total cost function may be determined, and it is shown as Equation (5) in the following way:

$$C_{Wind}(t) = 152.616 \times P_{Wind}(t) \tag{5}$$

For this study, Figure 3 shows a typical assumed generated power of the wind farm during a 24-hour period. This data isn't seasonal or regionally specific; it's just assumed for the sake of this experiment [22].

2.4 ESS

A battery with a capacity of 500 kWh was used for this investigation with a constraint that the daily number of cycles is fixed at 2. If the usage of ESS exceeds allowed number of cycles in each day, then it is automatically disconnected from the system. The minimum and maximum SOC of ESS are set to 10% and 90% respectively, initial SOC being 50%. The battery's cost function is obtained from Equations (2) and (3), much like the two prior DGs. It is expected that the I_P and O&M expenses per unit of produced energy (G^E) are 1000\$/kW and 1.6 cents per kilowatt hour [28]. Equation (6) was used to calculate the final cost function [26].

$$C_B(t) = 119 \times P_B(t) \tag{6}$$

Table 3 Constraints

Mode of Operation	Governing Equations	Action
Grid-connected	$P_{Grid} = P_{Gen} - P_{Load}; P_{Grid} > 0$	Buy
	$P_{Grid} = P_{Gen} - P_{Load}; P_{Grid} < 0$	Sell
Islanded	$P_{Gen} = P_{Load};$	–

2.5 Constraints

Constraints functions are employed to aid the system in achieving its goals. Grid-connected mode allows the MG to purchase or sell power from or to the main grid based on load. If the power generated by the DGs does not match the power necessary to satisfy the load, then electricity purchased from or sold to the grid equals the difference between the power generated and the demand for the load. When the MG is in islanded mode, it is not connected to the main grid, hence there is no way to buy or sell power during this mode.

3 Methodology – Optimization Algorithms

This section introduces the novel optimization which is based on the outstanding behavior of swarm intelligence and cuckoo bird search capabilities. Details of HFPSOCS algorithm and its implementation to discover the most optimal solution set to the chosen microgrid problem are presented.

3.1 Overview of Particle Swarm Optimization (PSO)

PSO is one of the widely implemented meta-heuristic algorithms in various fields because of ease of implementation and faster convergence towards an optimal solution set. It is a population-based optimization algorithm discovered by Kennedy and Eberhart in 1995. This meta-heuristic algorithm uses swarm intelligence consisting of particles or swarms. Each swarm is cognate with position and velocity vectors, namely x_{ij} and y_{ij}. The dimension of the search space determines the size of these vectors. The PSO, much like other evolutionary algorithms, initializes a swarm (a set of candidate solutions) and then searches for the best possible global optimum. It considers several particles to be potential solutions and each particle moves across the search space at a certain velocity to locate the optimal candidate set. The term P_{LBest} refers to the best local solution that a particle has come up with as iterations go on. The P_{LBest} that is superior to all the other particles is referred to as the P_{GBest}. Each particle must consider its current location, its current velocity,

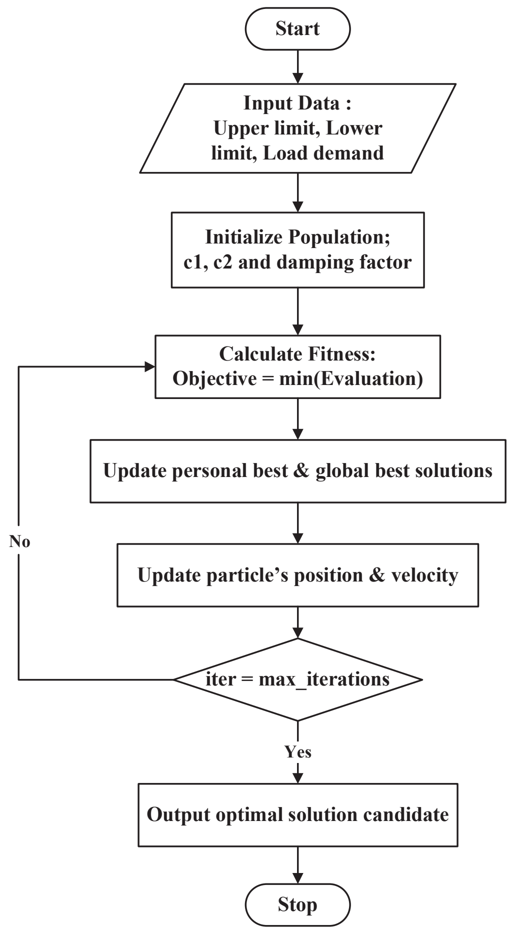

Figure 4 Flowchart of PSO algorithm.

and the distance to local best and global best before it can update its position. Each particle attempts to improve by mimicking successful peers. The best place in the search space that each particle has ever visited may also be stored in its memory [20, 23].

$v_{pop}(t)$ is used to determine the velocities of the particles after each iteration. After that, $X_{pop}(t)$ is used to determine where the particle position is updated to. Until a stopping criterion is reached, the particle position keeps changing. The flowchart (Figure 4) defined in Table 5 gives a step-by-step approach to the algorithm.

Table 4 Pseudocode breakdown of PSO

Pseudo code of the PSO Algorithm:
Begin Process
Initialization
A. Params:
C1: Cognitive component
C2: Social component
W: Inertia factor
W_{damp}: Damping factor
Np: Swam population size
B. Generate initial swarm using randomly uniformly distributed function
C. Evaluate fitness function
Main Loop
for $(iter = 1,\ iter\ \leq iter_{max},\ iter++)$ **do**
for $(pop = 1, pop \leq N_p,\ pop++)$ **do**
//Evaluate particle velocity
$v_{pop}(t) = w * v_{pop}(t-1)+$
$c_1 * r_1 * (P_{LBest} - (t-1))+$
$c_2 * r_2 * (P_{GBest} - X_{pop}(t-1))$
//Update particle position
$X_{pop}(t) = X_{pop}(t-1) + v_{pop}(t)$
if $f(X_{pop}) \leq f(P_{LBest})$ **then** $P_{LBest} = X_{pop}$
if $f(X_{pop}) \leq f(P_{GBest})$ **then** $P_{GBest} = X_{pop}$
Update X_{pop} & v_{pop}
end if
end if
end for
end for
Best Solution
End Process

3.2 Overview of Modified CSA

Inspired from the lifestyle and brooding behavior of the cuckoo bird, this algorithm was introduced by Xin-She-Yang and Suash Deb in 2009 [27]. Instead of using basic isotropic random-walks, Levy flights is used to improve the performance of the technique. The standard CSA uses the following three important rules, in solving an optimization problem:

- Each cuckoo bird picks a nest at random and lays one egg every time.
- The highest quality eggs (solutions) in the best nests will be passed down to the future generations of birds.
- Given that the number of host nests is invariable, the probability of discovering an egg laid by cuckoo bird in the host nest is $p_a \epsilon (0, 1)$; 1

Table 5 Pseudocode breakdown of MCS

Pseudo code of the MCS Algorithm:

Begin Process
Initialization
  a. Params:
     Np: Population Size
     max_iter: Maximum number of iterations
     $\mathrm{p_a}$: probability of discovery rate of alien eggs
     sigma: 0.6966, beta: 3/2
     a,b: Two positive random numbers, $\exists\, 0 < a < b < 1$
  b. Initialize swarm and evaluate fitness and update p_g
Main Loop
while (iterations <= max_iter) **do**
    for *i* from *1 to Np*: **do**
      //Calculate Self-Adaptive step size
      $\alpha_t = (b-a) * \frac{(e^{\frac{10*(t-1)}{t_M-1}} - 1)}{e^{10}-1}$
      //Update position by applying levy flights
      randomStep = findStep()
      $x_i(t+1) = x_i(t) \; + \; randomStep * (x_i(t) - p_g)$
      //Generate Gamma exemplar for $\mathrm{x_i}$
      gammaExemplar()
      // Update global best
        if $f(x_i) \leq f(p_g)$ **then** $p_g = x_i$
        end if
    end for
end while
Best Solution
End Process

being discovered. In this circumstance, the host bird has two options: either remove the egg from the nest or abandon the nest and construct an entirely new one.

For implementation, the following representation is adopted: each egg in a nest symbolizes a solution. The goal is to leverage new and superior options (cuckoo bird) to replace poorer quality solution/eggs. By controlling the switching parameter p_a, the local search random walk and global explorative capability. The equation to express local random walk is given as follows:

$$\sigma_u = \left(\frac{\Gamma(1+\beta) \times \sin(\pi + \frac{\beta}{2})}{\Gamma(\frac{(1+\beta)}{2}) \times \beta \times (2^{\frac{\beta-1}{2}})} \right)^{1/\beta} \; ; \; \sigma_v = 1 \tag{7}$$

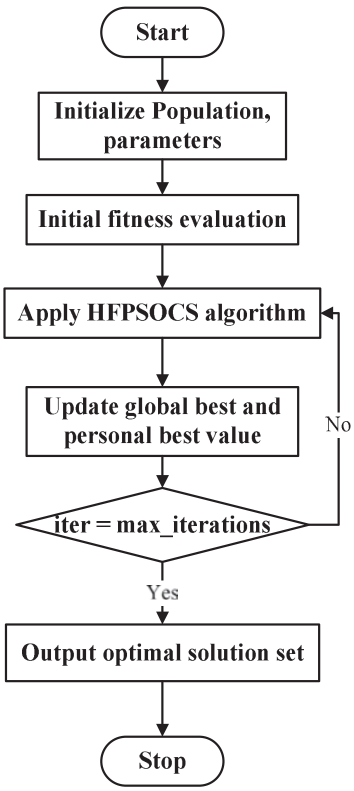

Figure 5 Flowchart of HFPSOMCS algorithm.

Also included are two search capabilities – local-search and global-search, which are governed by a switching probability and/or discovery probability. As mentioned in the earlier paragraph, the local-search (for $p_a = 0.25$) is relatively time-consuming, accounting for around one-fourth of the whole search time, whereas the global-search accounts for approximately three-fourths of the total search time. As a result, the global optimality can be found with a higher probability because of a more efficient global search [24].

The fact that it employs Lévy flights rather than normal random walks as part of its global search is an additional benefit of CSA. CSA can traverse the search space more efficiently than other meta-heuristic methods using the ordinary Gaussian process because Levy flights have an infinite mean and variance. The flowchart (Figure 5) defined in Table 6, gives a step-by-step approach to the algorithm.

Table 6 Benchmark functions with constraints

Function Name	Dimension	Problem	Variable Bounds	Global Minimum
Sphere Function	30	$f(x) = \sum_{i=1}^{d} x_i^2$	$x_i \in [-5.12, 5.12]$	$f(x^*) = 0,\ at\ x^* = (0, \ldots, 0)$
Rastrigin Function	30	$f(x) = 10d + \sum_{i=1}^{d} (x_i^2 - 10\cos(2\pi x_i))$	$x_i \in [-5.12, 5.12]$	$f(x^*) = 0,\ at\ x^* = (0, \ldots, 0)$

3.3 Overview of HFPSOMCS

The prime motivation behind the conceptualization and implementation of hybridized algorithm is that PSO can converge swiftly on the local best solution, though not always on the global best candidate set. According to some evaluations, it is implied that the mathematical equations used in PSO do not meet the global convergence criteria, and so there is no certainty of convergence to the global solution set. MCSA, on the other hand, has proven to satisfy the global convergence criterion and so ensures global convergence. This means that when it comes to solving multimodal optimization case studies, cuckoo search may generally converge to the optimality while PSO may converge to a local optimum set.

In contrast, MCSA takes several iterations to get the global best in the specified search space. A consequence of this is a significant increase in computing time, which is a disadvantage in scheduling applications. A novel feedback algorithm has been developed to achieve a balance between two desirable characteristics. Figure 6 illustrates the flow chart of the hybridization technique.

For the benchmark functions displayed in the table, the hybrid algorithm was used to optimize the performance of the system. The following table lists the parameters that were selected for use in the system. Traditional PSO and HFPSOMCS methods yielded the optimization results depicted in Figure 7. The hybrid algorithm outperformed PSO in both functions tested here. Afterwards, the hybrid system was used to resolve the EMS problem in the microgrid under consideration. After that, the findings and case studies are reviewed and developed more fully.

4 Case Studies & Results

In this section, the findings of EMS are discussed. Investigation is carried out for a day (24 hours operation) to determine the most efficient dispatch of the

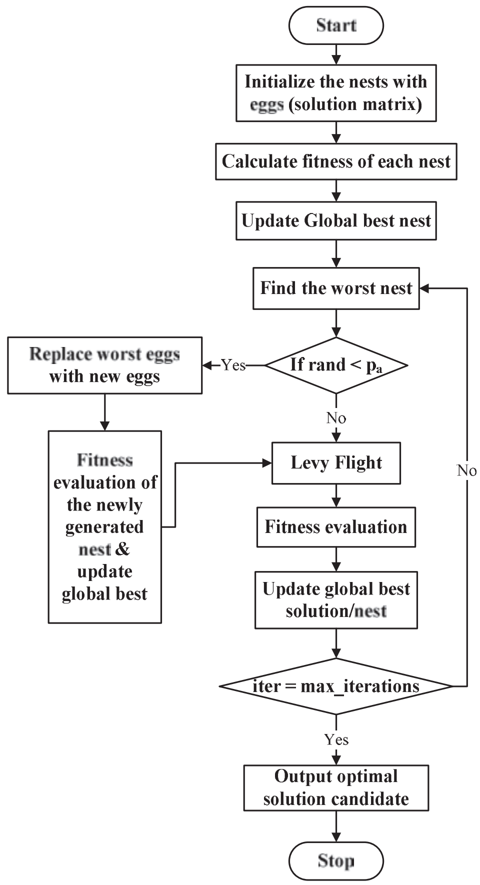

Figure 6 Flowchart of MCS algorithm.

DERs and utility grid. Microgrid is subjected to three different case studies, as follows:

1st Case Study	Grid Connected Mode	Summer season tariff rates
		Winter season tariff rates
2nd Case Study	Islanded/Standalone Mode	Summer season tariff rates
		Winter season tariff rates
3rd Case Study	Combined Mode (Grid + Islanded)	Summer season tariff rates
		Winter season tariff rates

Figure 11 depicts the load demand for a 24-hour time, which was utilized for all the case studies. There is a large difference in load demand between

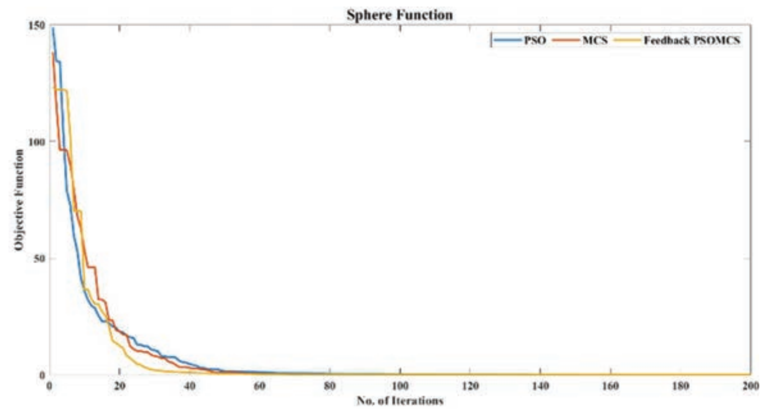

Figure 7(a) Three algorithms' performance on the sphere function.

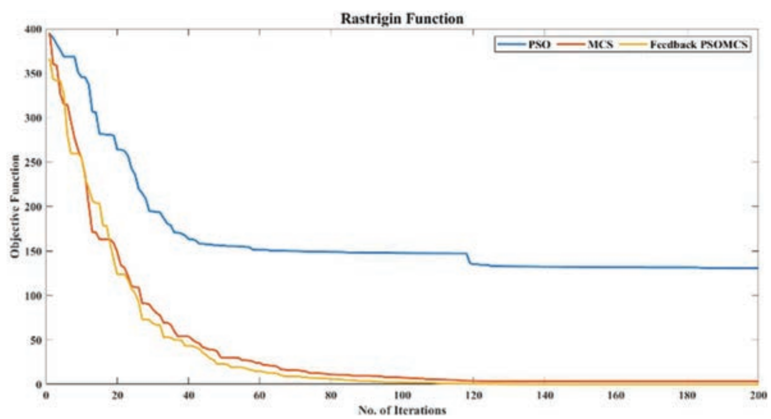

Figure 7(b) Three algorithms' performance on the Rastrigin function.

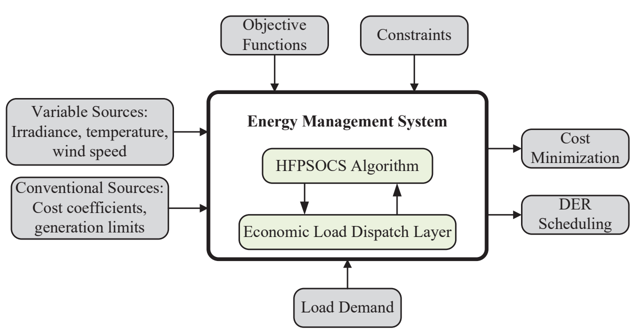

Figure 8 EMS architecture.

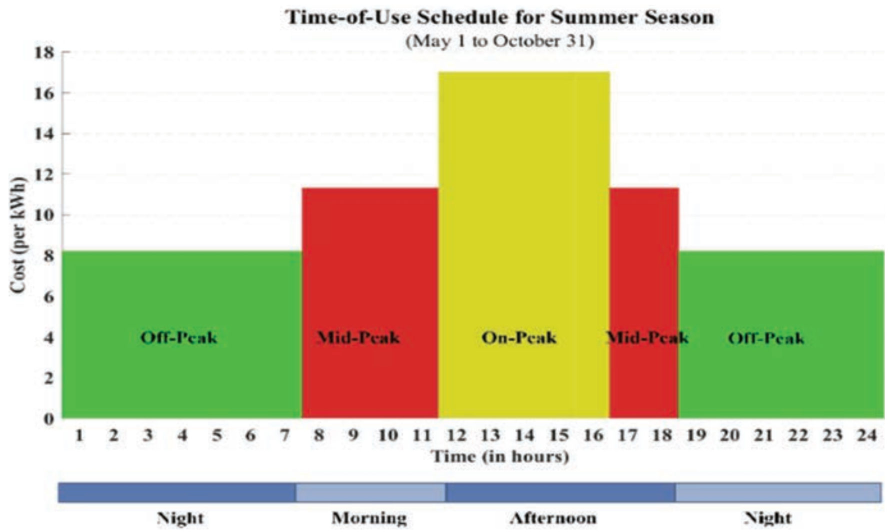

Figure 9 Main grid tariff for summer season.

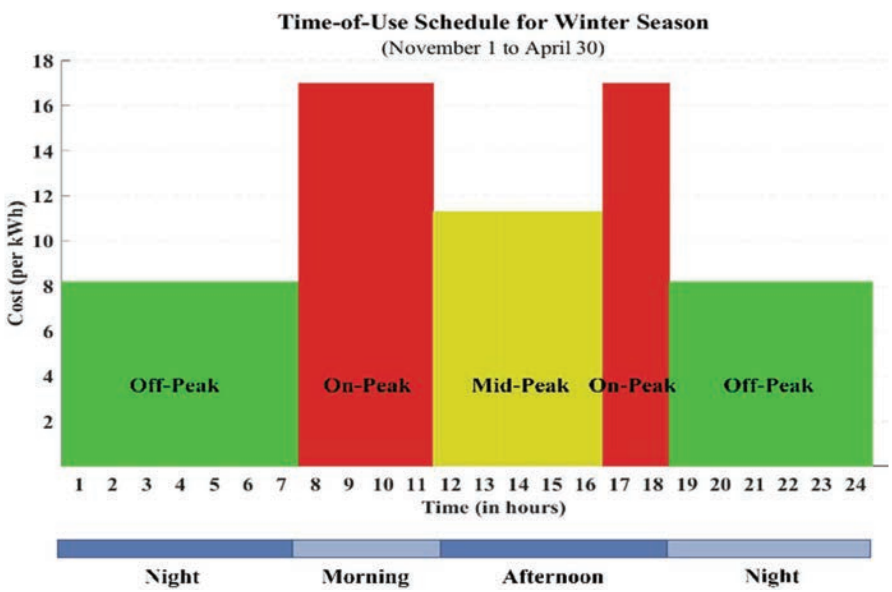

Figure 10 Main grid tariff for winter season.

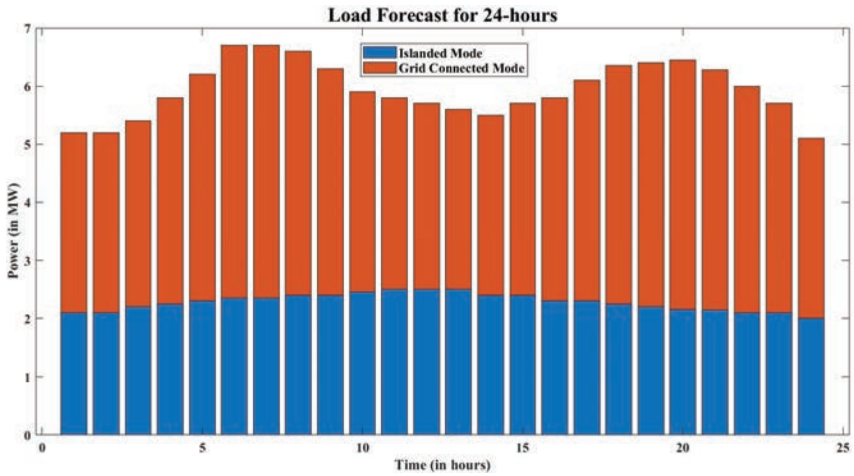

Figure 11 Load demand forecast for a 24-hour period.

the islanded mode and the grid connected mode, as seen in the Figure 11. As a result, load shedding is necessary, and the system only provides power to vital loads while the system enters standalone mode.

The main grid tariff is obtained from the website of the Oshawa PUC, with tariffs effective November 2021 [25]. The case studies are carried out during both the summer and winter seasons, with the primary goal of understanding BESS participation and the secondary goal of investigating the interaction between the main grid and DG units. Figures 9 and 10 show time-of-use schedule for a 24-hour operation period dependent on operating circumstances. When it comes to Summer, there is a distinct midday peak hour. This is the busiest time of year for air conditioners. Early morning and evening are two of the busiest times of day in the winter. When it is cold outside, people tend to use more heating, lighting, and appliances in their homes.

4.1 1st Case Study: Grid-connected Mode

All the system's power needs are covered by the DG units, ESS, and the main grid in this mode.

CHP, Diesel generator, Natural gas generators, Wind, Solar, Energy Storage Systems (ESS), and the main grid are all examined in this case study during a 24-hour operating period. Load demand, main grid tariff, and wind and PV power availability are all taken into consideration in an optimal EMS

Table 7 MG's hourly operation cost breakdown (Case 1)

	Cost (in $)			Cost (in $)	
Hour	Summer	Winter	Hour	Summer	Winter
1	47.50	46.90	13	−2.54	14.59
2	7.30	6.10	14	3.65	13.94
3	15.79	14.88	15	28.44	40.90
4	46.38	46.38	16	58.38	64.90
5	86.99	87.08	17	96.46	96.46
6	113.92	116.30	18	116.09	150.99
7	122.74	124.97	19	127.84	170.68
8	134.10	175.17	20	105.70	108.10
9	117.53	125.59	21	92.58	94.50
10	169.68	169.30	22	72.90	74.10
11	65.21	26.40	23	48.30	48.60
12	15.02	29.92	24	7.30	6.10

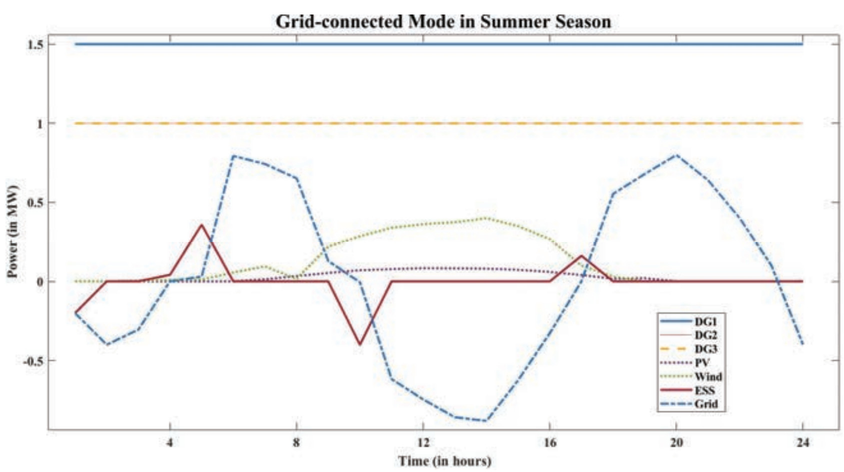

Figure 12 EMS optimum dispatch for grid-connected mode with summer tariff.

model. In addition, it is assumed that all the generators are running, and the objective of the optimization algorithm is to identify the approach that results in the lowest possible operating cost while still satisfying the demand for electricity. Table 7 and Figures 12 & 13 summarize the findings of this case study in both seasons.

Figures 12 & 13 shows the EMS in grid-connected mode at its optimum output. The algorithm was able to discover the best way to deploy DGs to

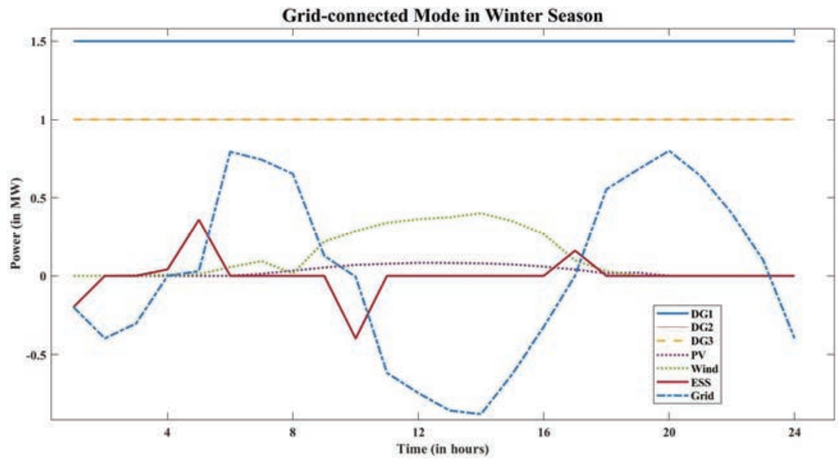

Figure 13 EMS Optimum Dispatch for Grid-connected mode with winter tariff.

meet the given demand during the time period. System purchases and sells electricity from the grid during both off-peak and peak periods. The total cost of operation over a day with summer tariff is \$1690.03 whereas with winter tariff is \$1852.95.

Table 7 breaks down the MG's hourly operational costs. When demand is lower than production, as shown in the table, operating costs are lower than those experienced when demand is higher (5–9 & 17–23). As a result, MG may save money by selling excess power back to the main grid. Similarly, if output falls short of demand, the utility must pay additional fees for power from the main grid. This indicates that the algorithm can make decisions about when to purchase and sell power to and from the main grid, which is beneficial for the system. The convergence trend for three different algorithms—namely, PSO, MCS, and HFPSOMCS—is depicted in a single graph in Figure 14. Because it can bring together the excellent search capabilities of MCS in tandem with the quicker convergence feature of PSO, the hybrid algorithm is able to converge at a faster rate than the other two optimization algorithms, as can be observed. The reason for this is because the hybrid algorithm was designed to maximize efficiency.

4.2 2nd Case Study: Islanded Mode

A more advanced EMS has been installed in an MG to cut down on the amount of energy needed to cater the load for a whole day, just as was done in the previous investigation. In this situation, however, the MG has

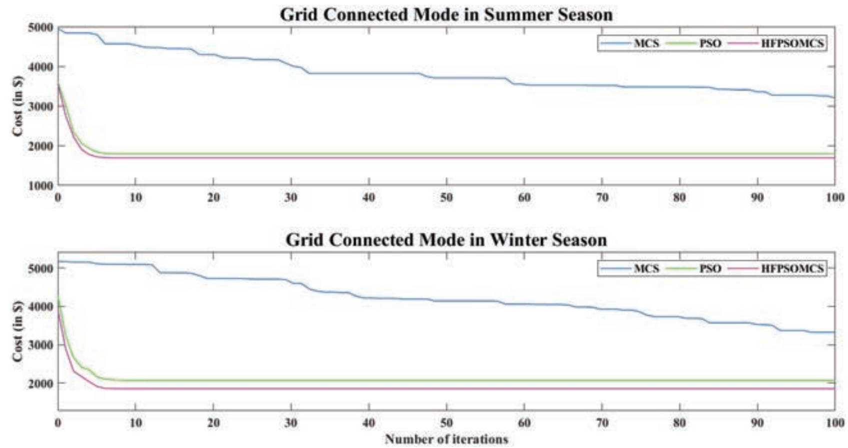

Figure 14 Cost convergence characteristics in grid-connected mode.

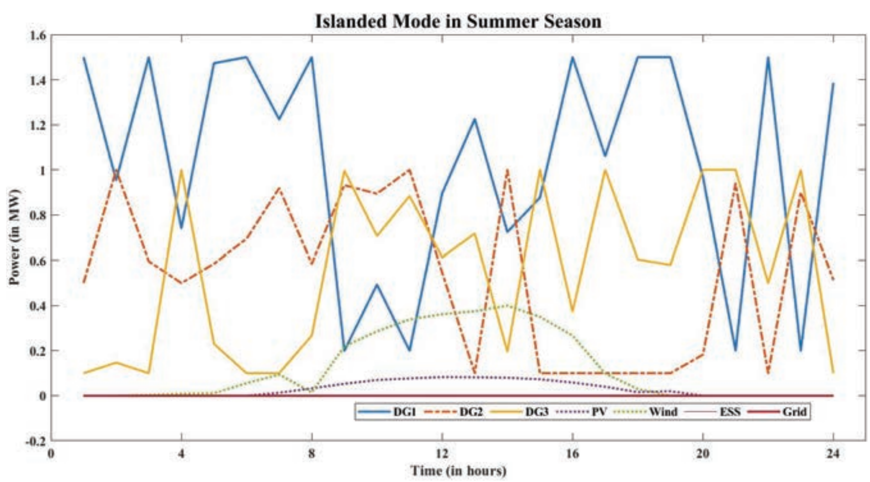

Figure 15 EMS optimum dispatch for islanded mode with summer tariff.

been separated from the main grid and is operating in an islanded state. Figure 11 illustrates the load requirement that was considered appropriate for this scenario. With no choice for power trading, this study's algorithm will be forced to choose the best strategy to dispatch three available generators. PV and Wind power plants are expected to be fully operational throughout each of these time periods.

The optimal output that the EMS was able to obtain for the islanded mode of operation is shown in Figures 15 & 16. The algorithm was able

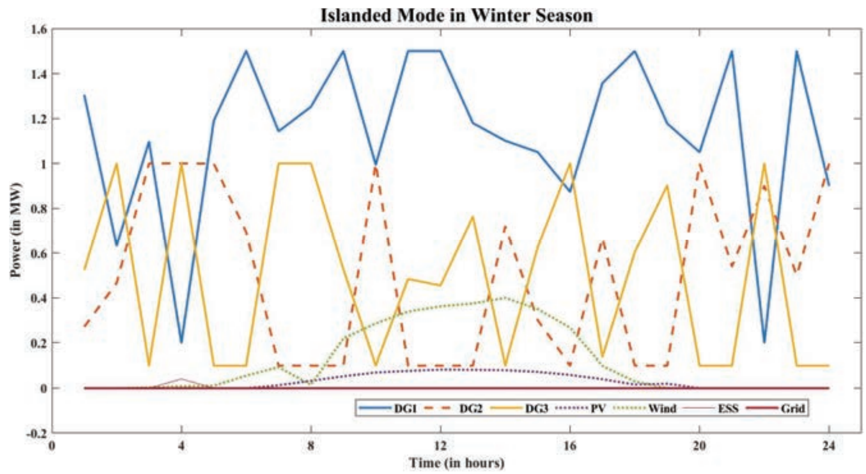

Figure 16 EMS optimum dispatch for islanded mode with winter tariff.

to determine the best way to distribute each generator so that it could meet the specified load requirement at each interval. For this scenario, the 24-hour total operating cost with summer tariff is \$1788.281. With winter tariff, the cost of operation is \$1792.92. The slight difference is due to the fact that the way DGs are fired up is entirely unidentical in both scenarios.

As can be seen in Table 8, the MG's operating costs when in islanded mode are broken down into discrete time intervals. In islanded mode, the system only provides power to essential loads, hence peak and off-peak hours were not significant for this case study's load demand. There is a noticeable difference in price between periods 9 and 16 hours, based on the data presented. All three generation sources—DGs, solar photovoltaics, and wind turbines—are operating at or near their full capacity because to the high demand for electricity. Figure 17 depicts the convergence of operational costs in this mode.

4.3 3rd Case Study: Combined Mode

In this situation, the MG system that is functioning in grid linked mode makes the transition into islanded mode for either a finite or an infinite amount of time. When it comes to everyday life, this kind of situation is not out of the question. The master controller, also known as the "brain" of the EMS, is responsible for turning off the power to the system's non-critical loads and isolating the main grid at the PCC when certain events occur, such as when

Table 8 MG's hourly operation cost breakdown (Case 2)

	Cost (in $)			Cost (in $)	
Hour	Summer	Winter	Hour	Summer	Winter
1	39.67	39.69	13	142.73	142.73
2	39.72	39.75	14	145.54	145.50
3	40.32	40.36	15	133.95	133.93
4	41.19	46.10	16	113.34	113.40
5	41.44	41.47	17	76.94	76.91
6	48.44	48.44	18	53.09	53.09
7	61.45	61.46	19	50.60	50.63
8	60.08	60.11	20	39.74	39.73
9	102.77	102.65	21	39.81	39.68
10	122.42	122.37	22	39.67	39.79
11	134.51	134.39	23	39.79	39.67
12	141.28	141.23	24	39.65	39.70

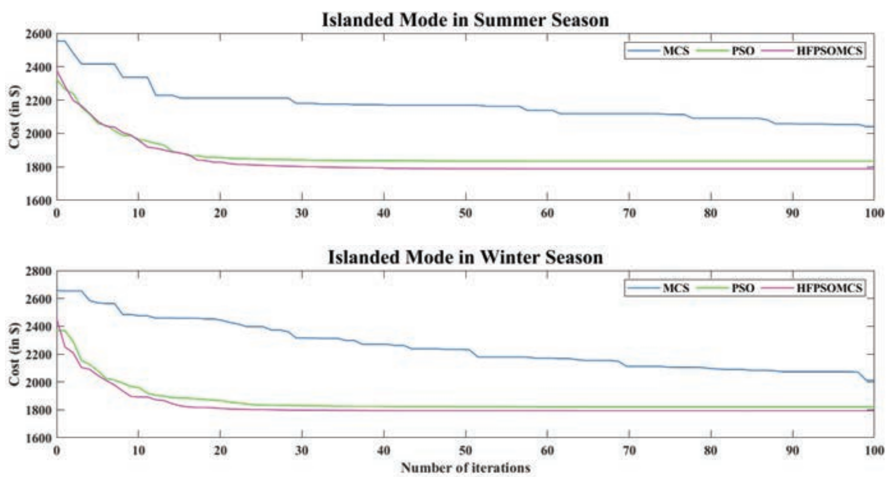

Figure 17 Cost convergence characteristics in islanded mode.

equipment fails, fuses blow, scheduled maintenance is performed, natural disasters occur, and so on.

The optimum outputs for dispatch are shown in Figures 18 & 19 when the system is operating in combined mode. The load is decreased to fifty percent as the system transitions from grid-connected mode to islanded mode between the fourteenth and fifteenth hours of the day. The cost of operation increases to $2005.30 when using the winter tariff, up from $1855.87 when using the summer rate. Because of the availability of power from PV and

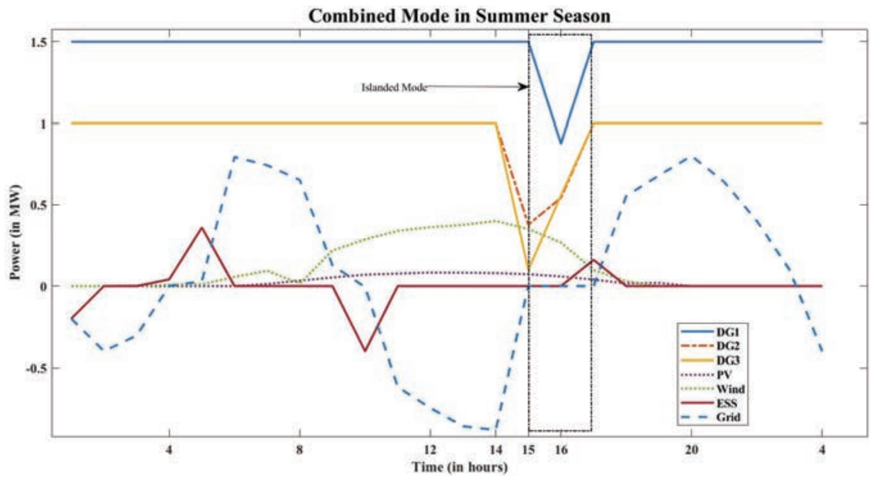

Figure 18 EMS optimum dispatch for combined mode with summer tariff.

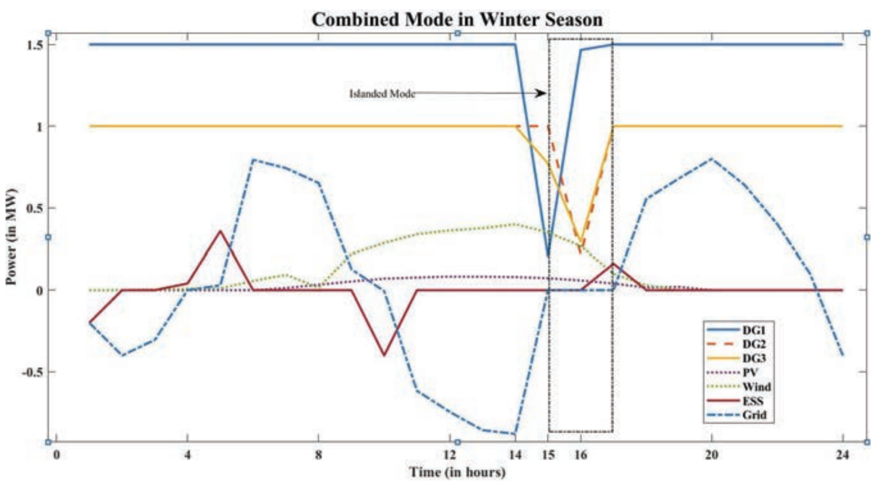

Figure 19 EMS optimum dispatch for combined mode with winter tariff.

wind farms in addition to the contribution of ESS, the generators are ramped up and down when in islanded mode. However, they do not operate at their full capacity because of the contribution of ESS.

The breakdown of the microgrid's costs, broken down by the hour, may be found in Table 9. Figure 20 depicts the convergence of operational costs in this mode.

Table 9 MG's hourly operation cost breakdown (Case 3)

Hour	Cost (in $) Summer	Cost (in $) Winter	Hour	Cost (in $) Summer	Cost (in $) Winter
1	47.50	46.90	13	−2.54	14.59
2	7.30	6.10	14	3.65	13.94
3	15.79	14.88	15	133.89	134.01
4	46.38	46.38	16	113.40	113.34
5	86.99	87.08	17	96.46	96.46
6	113.92	116.30	18	116.09	150.99
7	122.74	124.97	19	127.84	170.68
8	134.10	175.17	20	105.70	108.10
9	117.53	125.59	21	92.58	94.50
10	169.68	169.30	22	72.90	74.10
11	65.21	26.40	23	48.30	48.60
12	15.02	29.92	24	7.30	6.10

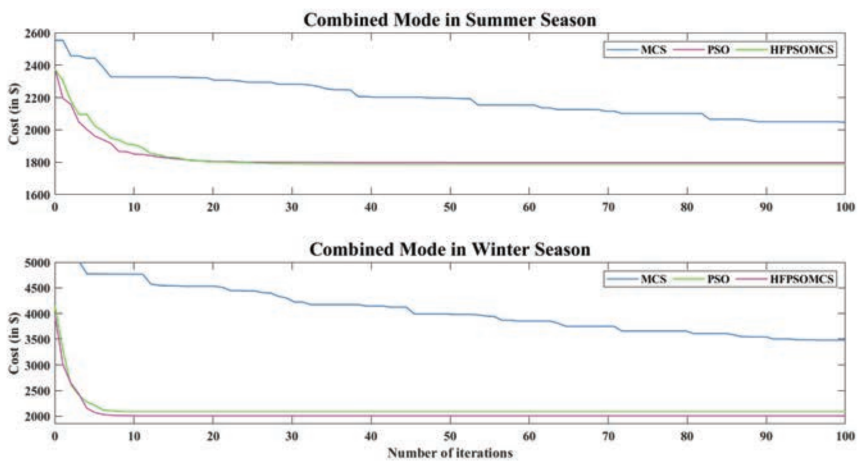

Figure 20 Cost convergence characteristics in combined mode.

5 Conclusion

This paper deals with an EMS to regulate the power flow, balance production to the demand, to keep the grid energy costs as low as possible using an optimization algorithm in a generic microgrid.

The microgrid is composed of a CHP plant, a natural gas generator, a diesel generator, a PV energy source, a wind energy source, and a battery energy storage system, as well as critical and non-critical loads. The microgrid can operate in grid-connected, islanded, or a combination of the first two modes. An AI-based EMS was developed using mathematical modelling of distributed energy sources and the main grid, and it can make decisions based on time-of-use and day-ahead forecasting. The cost functions are power and time dependent equations.

As described in Section 4, three algorithms, i.e., PSO, MCS, and HFPSOMCS, were implemented on three case studies for this research work. A robust feedback-based hybrid PSO-MCS optimization technique is developed with the goal of optimizing the EMS and improving battery life. By combining the best aspects of two different algorithms (PSO & MCS), the novel technique resulted in optimal scheduling and cost-saving solutions of energy management components in grid-connected, islanded, and combined modes of operation by adhering to the system's limits.

When compared to PSO and MCS, the implementation of the novel algorithm resulted in a reduction of 6%, 9%, and 2.5%, respectively, in the cost of operation and maintenance for grid-connected, combined, and islanded modes of operation throughout the summer season. In a similar vein, the costs of operation and maintenance dropped by 11%, 2%, and 4%, respectively, throughout the winter season in grid-connected, combined, and islanded modes of operation, respectively. As PSO's functionalities were added, the convergence of hybrid feedback PSO-MCS increased by 8%, resulting in lower microgrid running costs. Convergence occurred in under 10 seconds on average during Python code execution.

In the future, machine learning can be integrated into the system to obtain more precise predictions of solar and wind factors (such as irradiance, cloud cover, wind speed, and so on), and cloud computing can be used to make judgments based on past data of these aspects.

References

[1] W. Yuan, Y. Wang, D. Liu, F. Deng and Z. Chen, "Impacts of Inductor Nonlinear Characteristic in Multiconverter Microgrids: Modeling, Analysis, and Mitigation," in IEEE Journal of Emerging and Selected Topics in Power Electronics, vol. 8, no. 4, pp. 3333–3347, Dec. 2020.

[2] Q. Jiang, M. Xue and G. Geng, "Energy Management of Microgrid in Grid-Connected and Stand-Alone Modes," in IEEE Transactions on Power Systems, vol. 28, no. 3, pp. 3380–3389, Aug. 2013.

[3] I. U. Nutkani, P. C. Loh, P. Wang and F. Blaabjerg, "Decentralized Economic Dispatch Scheme with Online Power Reserve for Microgrids," in IEEE Transactions on Smart Grid, vol. 8, no. 1, pp. 139–148, Jan. 2017.

[4] I. U. Nutkani, P. C. Loh and F. Blaabjerg, "Droop Scheme with Consideration of Oper-ating Costs," in IEEE Transactions on Power Electronics, vol. 29, no. 3, pp. 1047–1052, March 2014.

[5] Carvallo, Juan, Schnitzer, Daniel, Lounsbury, Deepa, Deshmukh, Ranjit, Apt, Jay and Kammen, Daniel. (2014). Microgrids for Rural Electrification: A critical review of best practices based on seven case studies.

[6] Aftab Ahmad Khan, Muhammad Naeem, Muhammad Iqbal, Saad Qaisar, Alagan Anpalagan, "A compendium of optimization objectives, constraints, tools and algorithms for energy management in microgrids," Renewable and Sustainable Energy Re-views, Volume 58, 2016, Pages 1664–1683, ISSN 1364-0321.

[7] J. Raya-Armenta, N. Bazmohammadi, J. Avina-Cervantes, D. Saez, J. Vasquez, and J. Guerrero, "Energy management system optimization in islanded microgrids: An over-view and future trends," Renew. Sustain. Energy Rev., vol. 149, pp. 1–20, Dec. 2021.

[8] K. Zhou, S. Yang, Z. Chen, and S. Ding, "Optimal load distribution model of microgrid in the smart grid environment," Renew. Sustain. Energy Rev., vol. 35, pp. 304–310, Jul. 2014.

[9] V. V. S. N. M. Vallem and A. Kumar, "Retracted: Optimal energy dispatch in microgrids with renewable energy sources and demand response," Int. Trans. Electr. Energy Syst., vol. 30, no. 5, pp. 1–27, May 2020.

[10] S. A. Arefifar, Y. A.-R. I. Mohamed, and T. H. M. EL-Fouly, "Optimum microgrid de-sign for enhancing reliability and supply-security," IEEE Trans. Smart Grid, vol. 4, no. 3, pp. 1567–1575, Sep. 2013.

[11] J. Sachs and O. Sawodny, "A two-stage model predictive control strategy for economic diesel-PV-battery island microgrid operation in rural areas," IEEE Trans. Sustain. Energy, vol. 7, no. 3, pp. 903–913, Jul. 2016.

[12] M. Combe, A. Mahmoudi, M. H. Haque, and R. Khezri, "Cost-effective sizing of an AC mini-grid hybrid power system for a remote area in South Australia," IET Gener., Transmiss. Distrib., vol. 13, no. 2, pp. 277–287, Jan. 2019.

[13] S. Ferahtia, A. Djeroui, H. Rezk, A. Houari, S. Zeghlache, and M. Machoum, "Optimal control and implementation of energy management strategy for a DC microgrid," Energy, vol. 238, Jan. 2021, Art. no. 121777.

[14] A. Maulik and D. Das, "Optimal power dispatch considering load and renewable generation uncertainties in an AC–DC hybrid microgrid," IET Gener., Transmiss. Distrib., vol. 13, no. 7, pp. 1164–1176, Apr. 2019.
[15] A. Kumar, M. Alaraj, M. Rizwan and U. Nangia, "Novel AI Based Energy Management System for Smart Grid with RES Integration," in IEEE Access, vol. 9, pp. 162530–162542, 2021.
[16] A. Zakariazadeh, S. Jadid, and P. Siano, "Smart microgrid energy and reserve scheduling with demand response using stochastic optimization," Int. J. Electr. Power Energy Syst., vol. 63, pp. 523–533, Dec. 2014.
[17] V. Bui, A. Hussain, and H.-M. Kim, "A multiagent-based hierarchical energy management strategy for multi-microgrids considering adjustable power and demand response," IEEE Trans. Smart Grid, vol. 9, no. 2, pp. 1323–1333, Mar. 2018.
[18] X. Li and S. Wang, "Energy management and operational control methods for grid battery energy storage systems," in CSEE Journal of Power and Energy Systems, vol. 7, no. 5, pp. 1026–1040, Sept. 2021.
[19] Y. Li, P. Wang, H. B. Gooi, J. Ye and L. Wu, "Multi-Objective Optimal Dispatch of Microgrid Under Uncertainties via Interval Optimization," in IEEE Transactions on Smart Grid, vol. 10, no. 2, pp. 2046–2058, March 2019, doi: 10.1109/TSG.2017.2787790.
[20] Zwe-Lee Gaing, "Particle swarm optimization to solving the economic dispatch considering the generator constraints," in IEEE Transactions on Power Systems, vol. 18, no. 3, pp. 1187–1195, Aug. 2003.
[21] N. Augustine, S. Suresh, P. Moghe, and K. Sheikh, "Economic dispatch for a microgrid considering renewable energy cost functions," 2012 IEEE PES Innov. Smart Grid Technol., pp. 1–7, 2012.
[22] M. Bhoye, S. N. Purohit, I. N. Trivedi, M. H. Pandya, P. Jangir and N. Jangir, "Energy management of Renewable Energy Sources in a microgrid using Cuckoo Search Algorithm," 2016 IEEE Students' Conference on Electrical, Electronics and Computer Science (SCEECS), Bhopal, 2016, pp. 1–6.
[23] Premalatha, Kandasamy & Natarajan, A. (2009). Hybrid PSO and GA for global maximization. Int J Open Prob Compt Math. 2.
[24] J. Zhao, S. Liu, M. Zhou, X. Guo and L. Qi, "Modified cuckoo search algorithm to solve economic power dispatch optimization problems," in IEEE/CAA Journal of Automatica Sinica, vol. 5, no. 4, pp. 794–806, July 2018, doi: 10.1109/JAS.2018.7511138.

[25] "Time of Use," opuc.on.ca. http://www.https://www.opuc.on.ca/time-of-use/ (accessed: March. 15, 2022).
[26] Zwe-Lee Gaing, "Particle swarm optimization to solving the economic dispatch considering the generator constraints," in IEEE Transactions on Power Systems, vol. 18, no. 3, pp. 1187–1195, Aug. 2003.
[27] X. -S. Yang and Suash Deb, "Cuckoo Search via Lévy flights," 2009 World Congress on Nature & Biologically Inspired Computing (NaBIC), 2009, pp. 210–214.
[28] M. Y. Ali, F. Khan and V. K. Sood, "Energy Management System of a Microgrid using Particle Swarm Optimization and Wireless Communication System," 2018 IEEE Electrical Power and Energy Conference (EPEC), 2018, pp. 1–7.

Biographies

Priyadarshini Balasubramanyam received the B.Eng. degree in Electrical & Electronics Engineering from University College of Engineering, Osmania University, India in 2018. She is currently working towards the Master's degree in Electrical & Computer Engineering from Ontario Tech University, Canada. Her research interests include microgrids and its operation and control, energy management systems, optimization, and renewable energy.

Vijay K. Sood obtained his Ph.D. in Power Electronics from the University of Bradford, England in 1977. From 1969–76, he was employed at the Railway Technical Centre, Derby, U.K. From 1976–2007, he was a Senior Researcher at IREQ (Hydro-Québec Research Institute) in Montreal, Quebec. In 2007, he joined Ontario Tech University in Oshawa, Ontario where he is now the Chair of the Department of Electrical, Computer and Software Engineering.

He is a Member of the Professional Engineers Ontario, a Life Fellow of the Institute of Electrical and Electronic Engineers (IEEE), a Fellow of the Engineering Institute of Canada (EIC) and Emeritus Fellow of the Canadian Academy of Engineering (CAE). His research interests are in the monitoring, control and protection of power systems using artificial intelligence techniques. Dr. Sood has published over 200 articles, 10 book chapters and written two books on HVDC Transmission.